

Refractometric optical sensor based on tapered photonic crystal waveguide

G. S. KLIROS*, K. A. PAPAGEORGIOU

*Department of Aeronautical Sciences, Division of Electronics and Communication Engineering,
Hellenic Air-Force Academy, Dekeleia Attica GR-1010, Greece*

We report on the design of a refractometric optical sensor based on a tapered photonic crystal waveguide of air-holes with complete transverse-electric (TE) photonic band-gap (PBG). The plane-wave expansion (PWE) and finite-difference time-domain (FDTD) methods were employed in order to design the device and investigate its transmission spectra and sensitivity characteristics. The shift in the mode-cutoff wavelength due to change in the refractive index of fluids infiltrated the air-holes, is found to be approximately linear and hence extremely suitable for sensing applications. The use of a tapered photonic crystal reduces the coupling losses between the ridge-access waveguides and the photonic crystal so that a wide range of wavelengths before cutoff, are transmitted through the structure with only a very limited loss. Since it is silicon-based, the sensor can be easily implemented to design ultracompact all optical integrated circuits.

(Received June 16, 2010; accepted July 14, 2010)

Keywords: Integrated optics, Photonic crystals sensors, Tapered waveguides, Photonic band-gap, PWE method, FDTD method

1. Introduction

Integrated optical sensors has a high potential to be employed as a device in many areas such as microbiology, automotive, environmental safety, defence and aerospace technology. Their main advantages are immunity to electromagnetic interference, high compactness and robustness and prospects of mass production, and also they have fast responsivity and higher sensitivities when compared to Micro-Electro-Mechanical Systems (MEMS) [1]. In the last years, there has been a growing effort in the realization of active and passive photonic crystal waveguides (PCWs) as ultra-compact optical components and circuits, which can be integrated monolithically on a single chip [2,3]. PCWs have been studied extensively for several applications, including optical waveguides [4,5], wavelength division multiplexing and demultiplexing devices [6,7], modulators and switches [8,9], as well as sensors [10-12]. Photonic crystals (PC) are artificial optical materials with a periodic modulation of the refractive index. Depending on the exact periodic modulation, PCs may possess a photonic bandgap, i.e. a range of frequencies where light propagation is prohibited. [4]. The advantage of PC structures inside the wider family of periodic photonic structures, lies in the high contrast of the periodic modulation of the refractive index. Using PC technology, strong light confinement in compact structures can be designed in such a way that can allow for innovative methods to manipulate the guided light.

Recently, a wide range of photonic crystal (PC) sensing devices has been presented in the literature [13-16]. Planar PCWs in which the light is guided along defects, such as missing rows of holes can be designed to obtain a very high and spatially selective sensitivity to changes in refractive index. In particular, PCWs are based on vertical

light confinement using index guiding and confinement in the horizontal plane provided by the PC properties. The horizontal periodic structure is commonly manufactured by etching a triangular array of air holes, which provides a large photonic bandgap (PBG) for TE-polarized light. Removing one row of holes in a PC lattice creates a defect waveguide [4], which has the advantage of providing single-mode transverse waveguiding over a wide frequency range. Such PCWs are very interesting for optofluidic sensors since they have a large sensing range making it applicable within a broad dynamic change of refractive index extending from air to high viscous fluids.

In this paper we present the design and simulation of a refractometric sensor based on a tapered photonic crystal waveguide. The use of a tapered PCW [17] is beneficial for efficient coupling between the input/output ridge waveguide to the photonic crystal waveguide. The PBG computations have been done using the plane-wave expansion method (PWE). The transmission spectra of the PC sensor has been obtained with the help of finite-difference time-domain (FDTD) method, changing the refractive index of the fluid infiltrated in the holes of the PCW. Finally, we determine the sensitivity of our device by observing the shift in the mode-cutoff wavelength as a function of the change in refractive index of the fluid.

2. Device design and numerical method

Let us first consider a 2D triangular PC with air-holes drilled on a high index dielectric substrate. The lattice constant and the radius of air holes are represented by a and r , respectively. The dielectric material is assumed to be Si with a refractive index of 3.47 at the modern telecommunication wavelength of 1.55 μm which is

compatible with conventional CMOS technology. We consider only TE modes since the band diagram calculation shows a large complete PBG [1]. To extract the photonic band structure, we use the 2D plane wave expansion (PWE) method with Bloch boundary conditions in which $(2 \times 13 + 1)^2 = 729$ plane waves have been used. As it is seen from the obtained photonic bandgap map of Fig.1, in order to have the largest band gap, the best choice is $r/a = 0.43$. However, considering manufacturing problems and vertical loss in PC slabs, the radius of air holes should be smaller. The hole radius of $r/a = 0.32$ is widely used in the literature and will be used throughout this paper. Therefore, a lattice pitch $a = 387.5$ nm and a hole radius $r = 124$ nm, is obtained. The corresponding photonic and dispersion diagram is given in Fig. 2 where the existence of a complete TE-mode photonic gap is indicated by the shaded region.

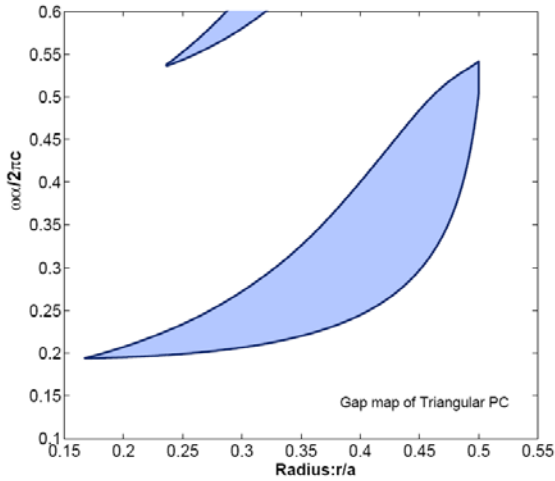


Fig. 1. The band gap map of triangular Si-PC of air holes.

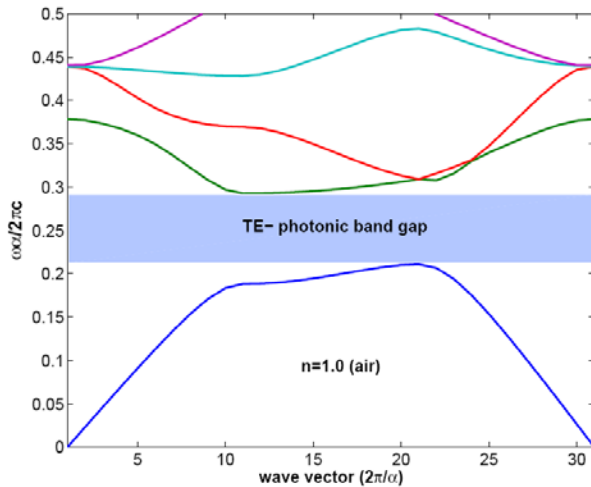


Fig. 2. TE band diagram of the triangular PCW of air holes with radius $r = 0.32a$ drilled in a high refractive index silicon with lattice constant $a = 387.5$ nm. The existence of PBG is indicated by the shaded region.

The PC waveguide is obtained by removing a single row of holes in the Γ -K direction of the PC and is $30a$ long with 16 rows of holes on each side of the line defect as it is shown in Fig. 3. In order to reduce the coupling losses between the ridge-access guides and the PC, a tapering technique is applied where the hole-radius, for the six last holes on each side of the line defect, is progressively reduced from $0.3a$ to $0.05a$. The proposed design gives rise to a large band gap for transverse-electric (TE) polarized light, with the fundamental PBG mode cutting off around $1.55 \mu\text{m}$ as is shown in Fig. 3. A very small excitation of TM-like modes may occur in the PCW due to the incoupling scheme, however these modes are not guided well near the edge of the TE-like band gap, so the potential crosstalk is very small [18].

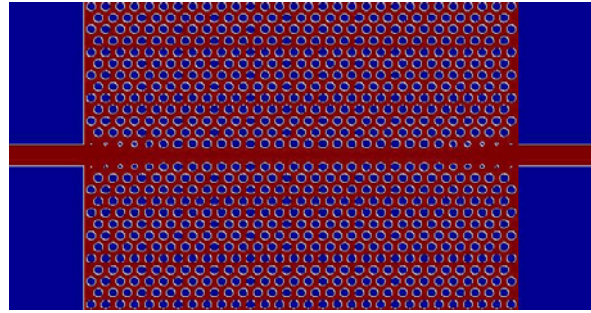


Fig. 3. Schematic diagram of the tapered PCW of air holes.

In order to investigate the proposed refractometric PC-sensor, we employed the well known 2D-FDTD method [19] based on the Yee's algorithm [20]. The electric and magnetic field components are evaluated at different grids having the same pitch but shifted over a half grid spacing, both in time (leapfrog algorithm in time) and space (staggered grid). Maxwell's equations in FDTD form for the TE-polarization are written as follows

$$E_x^{n+1}(i, j) = E_x^n(i, j) + \frac{\Delta t}{\varepsilon(i, j)} \frac{H_z^{n+1/2}(i, j+1/2) - H_z^{n+1/2}(i, j-1/2)}{\Delta y} \quad (1)$$

$$E_y^{n+1}(i, j) = E_y^n(i, j) + \frac{\Delta t}{\varepsilon(i, j)} \frac{H_z^{n+1/2}(i+1/2, j) - H_z^{n+1/2}(i-1/2, j)}{\Delta x} \quad (2)$$

$$H_z^{n+1/2}(i, j) = H_z^{n-1/2}(i, j) + \dots$$

$$\frac{\Delta t}{\mu(i, j)} \left[\frac{E_x^n(i, j+1/2) - E_x^n(i, j-1/2)}{\Delta y} - \frac{E_y^n(i+1/2, j) - E_y^n(i-1/2, j)}{\Delta x} \right] \quad (3)$$

where $\varepsilon(i, j)$ is the permittivity, $\mu(i, j)$ is the permeability at each grid point (i, j) . Here, we have considered the transverse electric (TE) mode polarization electric fields in

the plane and is normal to the axis of the air-holes. The spectrum of the power transmission is calculated in our code using 50,000 time steps and spatial step in both directions are fixed to $\Delta x = \Delta y = 0.05$. The relation between spatial and temporal steps satisfies the Courant's stability condition $\Delta t = 0.95 \Delta x / (\sqrt{2} c)$, where c is the speed of light in a vacuum [21]. The tapered PCW is connected efficiently to an input slab waveguide. A Gaussian source with central frequency and width matching that of the photonic band-gap is positioned in the middle of the input slab. As absorbing boundaries, we used the perfect matched layer (PML) widely adopted by many researchers [22]. The transmission is computed as the ratio of output and input powers obtained by integration of the Poynting vector fluxes at the detectors. To reduce computational effort, the effective index approximation [23] for the vertical direction is applied. For a suitable choice of effective refractive index, 2D simulations give the same quantitative characteristics as 3D simulations [24].

3. Results and discussion

To study the designed structure for sensing applications, the transmission spectra is calculated by means of the FDTD code. Fig. 4 shows the normalized transmission spectrum of the sensor when the lattice holes are filled with fluids of increasing refractive index. As it is seen, a wide range of wavelengths are transmitted through the structure with only a very limited loss. Peaks in the transmissions arise from the Fabry-Perot oscillations from the two boundaries. The interesting property is the sudden drop in transmission at the band edge around $1.55 \mu\text{m}$ where the transmission of the fundamental PBG-mode is no longer possible. This sharp drop in transmission (mode cutoff) indicates that the designed structure has potential applications in the sensing area.

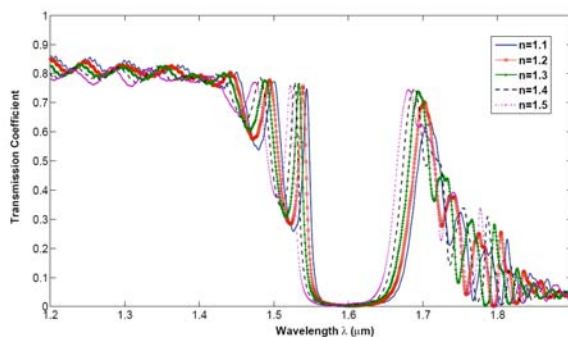


Fig. 4. Transmission spectra of the PC air-holes waveguide the air holes are filled by fluids with increasing refractive indices.

Fig. 5 shows the change in the transmission spectra when the air-holes are filled by fluids with refractive index of $n=1.0$, 1.1 , 1.2 , 1.3 , 1.33 (de-ionized water), 1.38 (butane gas), 1.4 , 1.48 , 1.5 and 1.52 (immersion oils). A

strong dependence of the mode-cutoff on the refractive index of the fluid is observed. It is worth noting that in all cases the maximum light transmission is about 0.77 at 'peak wavelength' that shifts to smaller wavelengths as the refractive index of the fluid increases.

Fig. 6 presents the cutoff wavelength shift ($\Delta\lambda_c$) as a function of the change in fluid refractive index infiltrated in the PCW-holes, where the reference wavelength is the cutoff wavelength for air. From the graph it is obvious that the cutoff wavelength shift is about 4.5 nm for change in refractive index $\delta n = 0.1$. Furthermore, the shift in the wavelength due to change in the refractive index of infiltrated fluid is found to be approximately linear and hence extremely suitable for sensing applications. It should be noted that, in order to obtain the curve in Fig. 5, the change in cutoff wavelength has been read out at a normalized transmission of 0.03.

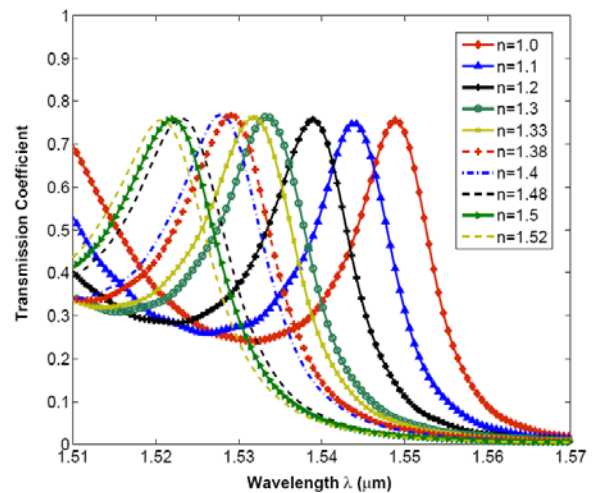


Fig. 5. Transmission spectra for different fluids in the wavelength range of interest in order to calculate the sensitivity curve of the refractometric sensor.

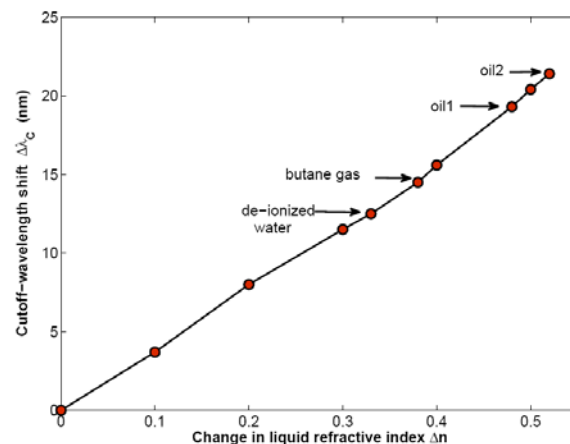


Fig. 6. Characteristic curve showing the simulated changes in cutoff wavelength versus changes in refractive index of fluid infiltrated the PCW holes.

4. Conclusion and future work

To conclude, we have designed and theoretically investigated a refractometric optical sensor based on tapered air-hole photonic crystal waveguides with complete transverse electric photonic band-gap. The use of tapered photonic crystal reduces the coupling losses between the ridge-access guides and the PC and a wide range of wavelengths before cutoff, are transmitted through the structure with only a very limited loss. The PWE method and FDTD simulation were employed in order to design the device and investigate its transmission spectra and sensitivity characteristics. For the working wavelength 1.55 μm , the transmission spectra has been calculated by changing the refractive index of the fluid in the air-holes and it has been found that a sudden drop in transmission occurs at the band edge around 1.55 μm where the transmission of the fundamental PBG-mode is no longer possible.

The wavelength position of this band edge (cutoff wavelength) is shifted to smaller wavelengths with increasing the refractive index. The shift in the cutoff wavelength due to change in the refractive index of infiltrated fluids is found to be approximately linear and hence extremely suitable for sensing applications. It should be noticed that, for a 2D photonic crystal waveguide, the electromagnetic field attenuates due to out-of-plane loss, but the shift of the wavelength mode-band edge tuned by the fluids is unaffected by the out-of-plane radiation. The simulation results show that the designed sensor is very sensitive to liquids or gases with small refractive index differences such as dry air, de-ionized water, butane gas, and immersion oils. Its sensitivity is mainly attributed to the strong dispersion of the PC mode. Since it is silicon-based, the designed sensor can be easily implemented to design ultra-compact all optical integrated circuits.

It should be possible to improve the refractive index response of the tapered-PC sensor by placing it in the sensing arm of a Mach-Zehnder interferometer (MZI) and exploiting the 'slow light' dispersion effect [25]. As is well known, the output signal becomes dependent on the cumulative phase difference between the two arms of MZI [26]. Near cut-off, the group velocity of the PCW-mode decreases dramatically, falling to zero at the mode cut-off. This wave compression can be utilized to design a compact device in which the required interaction length to produce a fixed phase shift is reduced by a factor c/v_g [8]. Integrated silicon photonic crystal modulators with reduced interaction length have already been proposed [8,9].

References

- [1] M. Notomi, NTT - Tech. Rev., **4**, 6 (2006).
- [2] W. Bogaerts, R. Baets, P. Dumon, V. Wiaux, S. Beckx, D. Taillaert, B. Luyssaert, J. V. Campenhout, P. Bienstman, D. Thourhout, J. Lightw. Technol. **23** (1), 401(2005).
- [3] S. Boutami, B. Bakir, J. Leclercq, X. Letartre, C. Seassal, P. Romeo, P. Regreny, M. Garrigues, P. Viktorovitch, IEEE J. Sel. Topics Quantum Electron. **13**(2), 244 (2007).
- [4] J. D. Joannopoulos, R. D. Meade, J. N. Winn, Photonic Crystals: Molding the Flow of Light, Princeton University Press, 1995.
- [5] C. G. Bostan, R. M. de Ridder, J. Optoelectron. Adv. Mater. **4**, 921 (2002).
- [6] A. D'Orazio, M. De Sario, V. Petruzzelli, F. Prudenziario, Opt. Express **11**, 230 (2003).
- [7] I. Sukhoivanov, I. Guryev, O. Shulika, A. Kublyk, O. Mashoshina, E. Alvaradaméndeza, J. A. Andrade-Lucio, J. Optoelectron. Adv. Mater. **8** (4), 1622 (2006).
- [8] Wei Jiang, L. Gu, X. Chen, R.T. Chen, Solid State Electronics **51**(10), 1278 (2007).
- [9] G. S. Kliros, A. N. Fotiadis, G. P. Tziopis, Optoelectron. Adv. Mater.-Rapid Commun. **3**(7) 655 (2009).
- [10] P. Domachuk, H.C Nguyen, B.J Eggleton, M Straub, M.Gu, Appl. Phys. Lett. **84**, 1838 (2004).
- [11] D. Erickson, T. Rockwood, T. Emery, A. Scheerer D. Psaltis, Opt. Lett. **31**, 5961 (2006).
- [12] N. Skivesen N, A. Têtu, M. Kristensen M, J. Kjems, L. H. Frandsen, P. Borel, Opt Express **15**(6), 3169 (2007).
- [13] S. Xiao S and N. A. Mortensen, J. Eur. Opt. Soc.-Rapid Pub. 106026 (2006).
- [14] S. Xiao, N. A. Mortensen, J. Opt. A: Pure Appl. Opt. **9**, S463 (2007).
- [15] D. Erickson, S. Mandal, A. Yang, B. Cordovez, Microfluidics and Nanofluidics **4**, 33 (2008).
- [16] F. Ouerghi, F. AbdelMalek, S. Haxha, R. Abid, H. Mejatty, I. Dayoub, J. Lightwave Technol. **27**(15), 3269 (2009).
- [17] P. Bienstman, S. Assefa, S. G. Johnson, J. D. Joannopoulos, G S. Petrich, L. A. Kolodziejski, J. Opt. Soc. Am. **B20**(9), 1817 (2003).
- [18] Y. Tanaka, T. Asano, R. Hatsuta, and S. Noda, J. Lightwave Technol. **22**, 2787 (2004).
- [19] A. Taflove, Computational Electrodynamics: The Finite-Difference Time-Domain Method 2nd edn., Norwood:Artech House, 2000.
- [20] S. K. Yee, IEEE Trans. Antennas Propag.. **14**(3), 302 (1966).
- [21] H. M. Masmoudi, M. A. Al-Sunaidi, J. M. Arnold, IEEE J. Lightwave Technol. **19**(6), 759 (2001).
- [22] J. P. A. Berenger, J. Comput. Phys. **114**, 185 (1994).
- [23] M. Qiu, B. Jaskorzynska, M. Swillo, H. Benisty, Microwave Opt. Technol. Lett., **34**(5), 387 (2002).
- [24] A. Lavrinenko, P.I. Borel, L.H. Frandsen, M. Thorhauge, A. Harpøth, M. Kristensen, T. Niemi, H. M. H. Chong, Opt. Express **12**, 234 (2004).
- [25] Toshihiko Baba, Nature Photonics **2**, 465 (2008).
- [26] B. J. Luff, J. S. Wilkinson, J. Piehler, U. Hollenbach, J. Ingenhoff, N. Fabricius, J. Lightwave Technol. **16**, 583 (1998).

*Corresponding author: gsksma@hol.gr